Proceedings of the 9th World Congress on Momentum, Heat and Mass Transfer (MHMT'24)
London, United Kingdom – April 11 – 13, 2024
Paper No. ENFHT 298
DOI: 10.11159/enfht24.298

Passive Vibration Reduction in Circular Cylinders: The Role of Slits

Ussama Ali[1], Md Islam[1], Isam Janajreh[1]
[1]Khalifa University of Science and Technology
Abu Dhabi, UAE
ussama.ali@ku.ac.ae; didarul.islam@ku.ac.ae; isam.janajreh@ku.ac.ae

Abstract – This work investigates a passive flow control method to mitigate vortex-induced vibration (VIV) by introducing a slit into a circular structure. The impact of varying slit sizes on the behaviour of a cylinder subjected to VIV is investigated across different reduced velocities (Ur) at a Reynolds number (Re) of 100. The size of the slit (S/D) is adjusted from 0 (without slit) to 0.1 & 0.2, where S corresponds to the width of slit & D the cylinder diameter. The mass and damping ratios are fixed at $m^* = 10$ and $\zeta = 0.005$, respectively, while Ur is varied from 2 to 10. The numerical analysis is conducted using Ansys/Fluent, incorporating mesh motion to consider cylinder vibration. The outcomes are presented in terms of vibration amplitude & frequency, drag & lift coefficients, Strouhal number, and vorticity contours. The findings suggest that the slit reduces lift and drag coefficients, effectively suppressing VIV. Examining maximum vibration amplitude, a 10% slit results in a 5.16% decrease, whereas a 20% slit leads to a substantial 34.27% reduction compared to a solid cylinder.

Keywords**:** Elastically mounted cylinder; Vortex-induced vibrations; Passive flow control; Slit effect; Lift & Drag; Computational fluid dynamics (CFD).

1. Introduction

The phenomenon of vortex-induced vibrations (VIV) has long been a subject of interest and concern in engineering and fluid dynamics, particularly when considering the structural integrity of cylindrical bodies exposed to flowing fluids [1]. VIV refers to the oscillations induced in a structure due to the unsteady shedding of vortices in its wake [2], [3], a phenomenon that can lead to fatigue and potential structural failure [4], [5]. To address this challenge, engineers and researchers have explored various strategies for mitigating VIV, and one such promising avenue is the use of passive control techniques [6]. Among these techniques, the incorporation of slits into cylindrical structures has emerged as a noteworthy and effective means of controlling vortex-induced vibrations [7].

Passive control methods are particularly appealing in fluid dynamics because they harness naturally occurring phenomena to modify the flow around a structure, mitigating undesirable effects without the need for active energy input [8]–[11]. In the context of vortex-induced vibrations, passive control techniques seek to alter the characteristics of the vortex shedding process, thereby reducing the forces and vibrations experienced by the structure [12]–[14]. The introduction of slits, or openings, in a cylindrical structure represents a subtle yet powerful approach to achieve this control [15]. The essence of the passive control technique involving slits lies in its ability to influence the fluid flow around the body, disturbing the formation of vortexes and subsequently mitigating the induced oscillations [16]. The slits act as flow modifiers, introducing deliberate disturbances that interact with the vortices in the wake, altering their characteristics and, in turn, minimizing the adverse effects of VIV [17].

Slits in a circular cylinder passively control vortex-induced vibrations, with crucial parameters being slit angle and slit width. Previous research [18] found that for a stationary slitted cylinder, an inclination angle of 30° maximizes lift force, with a decrease beyond 30° due to reduced flow within the slit. Drag is minimized at 0° inclination, increasing until 60° and then remaining constant. The horizontal slit outperforms other angles in terms of least drag and lift. Verma et al. [19] explored diverging and converging slit nozzles at Re = 500, with the parallel slit proving most effective. Baek and Karniadakis [20] found optimal slit width ratio (S/D) to be 0.16 at Re = 500 and 0.12 at Re = 1000. Karasu [21] implemented slits on a diamond structure at $Re = 8.6\times10^3$, finding weak suppression at S/D = 0.07 and reduced shear layer thickness with increased slit width. Igarashi [22] studied the effect of slit at high Reynolds numbers (13.8×10^3 to 52×10^3), observing injection flow for 0° to 40° and boundary layer interaction for 60° to 90° slit inclination. Another study [23] found that larger slits at higher Reynolds

numbers increase drag and vortex shedding frequency. In another work, Mishra and De [24] examined the flow within the slit for Reynolds numbers varying between 100 and 500. They tested slits with S/D ≤ 0.25, and reported that for Re < 300, periodic vortex shedding occurs for all slit sizes, while for Re higher than 300, and S/D greater than 0.15 irregular vortex shedding appear in the wake.

The exploration of passive control techniques, specifically the incorporation of slits, presents a compelling avenue for mitigating vortex-induced vibrations in cylindrical structures exposed to fluid flow. The present study delves into the application and effectiveness of this technique to control vortex-induced vibrations in a circular structure. The investigation aims to reveal how varying the size of these slits influences the behaviour of a cylinder subjected to flow-induced vibrations. This exploration is conducted across different reduced velocities (Ur) at Re = 100. This study systematically adjusts slit width ratio, examining the impact of this variation on critical parameters such as vorticity, drag & lift, and vibration frequency & amplitude. The methodology, findings, and implications for practical applications are discussed in subsequent sections.

2. Numerical Method

2.1. Problem Description

As shown in Fig. 1, the considered problem involves the interaction of an elastically mounted cylinder with external fluid flow, where the cylinder has a diameter (D) and moves exclusively in crossflow direction. Flow is considered laminar, incompressible, and transient. At Re equal to 100, the cylinder is subjected to the flow at various reduced velocities to assess the impact of a slit on both the amplitude & frequency of VIV. Fig. 1 illustrates a cylinder incorporated with a horizontal slit in line with the direction of flow. The diameter of the cylinder and the width of the slit are denoted as D and S, respectively. The computational setup encompasses a circular two-dimensional (2D) domain with the cylinder at its centre. The domain size is 50 times the cylinder diameter, ensuring a comprehensive capture of the downstream vortex-shedding pattern. To prevent domain boundaries from affecting the cylinder response, a blockage ratio of 2% is maintained in the computational domain [25], [26]. Fluid forces are linked to transverse (y-direction) displacement of the cylinder using a user-defined function (UDF), enabling one-degree-of-freedom oscillation. Ansys Fluent employs "smoothing dynamic mesh technique" for cylinder oscillations. Second-order upwind methods are used for solving the continuity and momentum equations, with convergence criteria of 1×10^{-6}. The runs continue until recurring periodic patterns are noted in drag and lift coefficients, along with transverse vibration. In transient analysis, the time step is chosen in such a way that the Courant–Friedrichs–Lewy (CFL) number ≤ 1, ensuring accuracy and stability [27]. The Reynolds number is kept constant at Re = 100 by keeping a fixed inlet velocity in the streamwise direction. The outlet side implements a free boundary condition with zero gage pressure. The structure is treated as a rigid body, and the surface of the cylinder is imposed to a no-slip boundary condition. For numerical analysis, damping ratio (ζ) is chosen as 0.005 and mass ratio (m*) is set at 10.

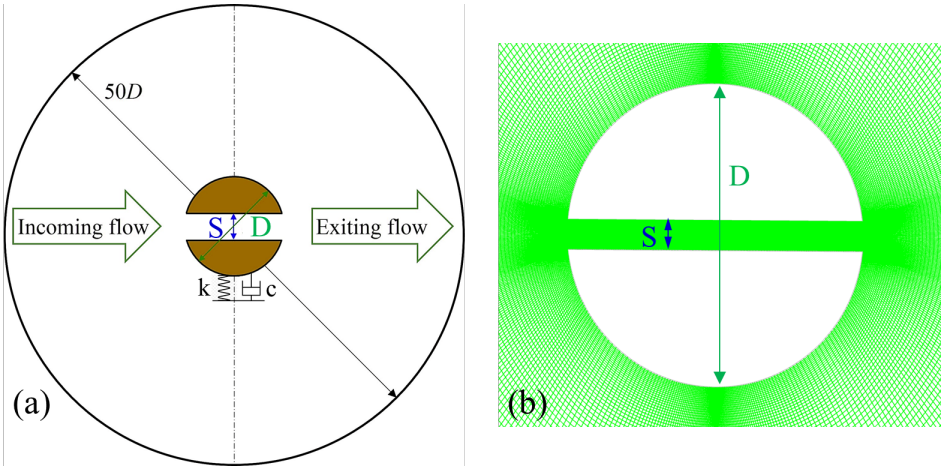

Fig. 1: (a) Visualization of the flow domain, and (b) discretized mesh for a slitted cylinder.

2.2. Mathematical Formulation

The Navier-Stokes equations govern fluid flow, comprising the conservation of mass and momentum in the planar direction, disregarding the influence of gravity. Thus, the 2D governing equations take the form:

$$\frac{\partial u_j}{\partial x_j} = 0 \tag{1}$$

$$\left[\frac{\partial \rho u_j}{\partial t} + \frac{\partial \rho u_j u_i}{\partial x_i}\right] = -\frac{\partial P}{\partial x_j} + \frac{\partial}{\partial x_i}\left[\mu\left[\frac{\partial u_j}{\partial x_i} + \frac{\partial u_i}{\partial x_j}\right]\right] \tag{2}$$

The initial two components in the momentum equation (Eq. 2) denote local and advective acceleration, whereas the final component signifies viscous forces. The lateral displacement of the cylinder is calculated from the following equation:

$$m\ddot{Y} + c\dot{Y} + kY = F_L \tag{3}$$

The damping coefficient (c) and the natural frequency (f_n) of the cylinder is given by:

$$c = 2\zeta\sqrt{km} \tag{4}$$

$$f_n = \frac{1}{2\pi}\sqrt{\frac{k}{m}} \tag{5}$$

The dimensionless quantities are expressed as:

Reynolds number, $$Re = \frac{U_\infty D}{\upsilon} \tag{6}$$

Reduced velocity, $$Ur = \frac{U_\infty}{f_n D} \tag{7}$$

Lift coefficient, $$C_L = \frac{2F_L}{\rho U_\infty^2 D} \tag{8}$$

Mass ratio, $$m^* = \frac{m_{cylinder}}{m_{fluid}} \tag{9}$$

2.3. Model Validation

In exploring the vibrational dynamics of a solid cylinder, the dimensionless vibration amplitude (Y/D) and the normalized vibration frequency (fy/fn) are matched to the work of Wanderley & Soares [28], as visually represented in Fig. 2. The structural characteristics are defined by m* = 1.88 and ζ = 0.00542, maintaining a Reynolds number of 100. Fig. 2 presents a clear side-by-side comparison, confirming the consistency between our results and what is documented in the existing study. This strongly supports the dependability of the fundamental model used for subsequent investigation.

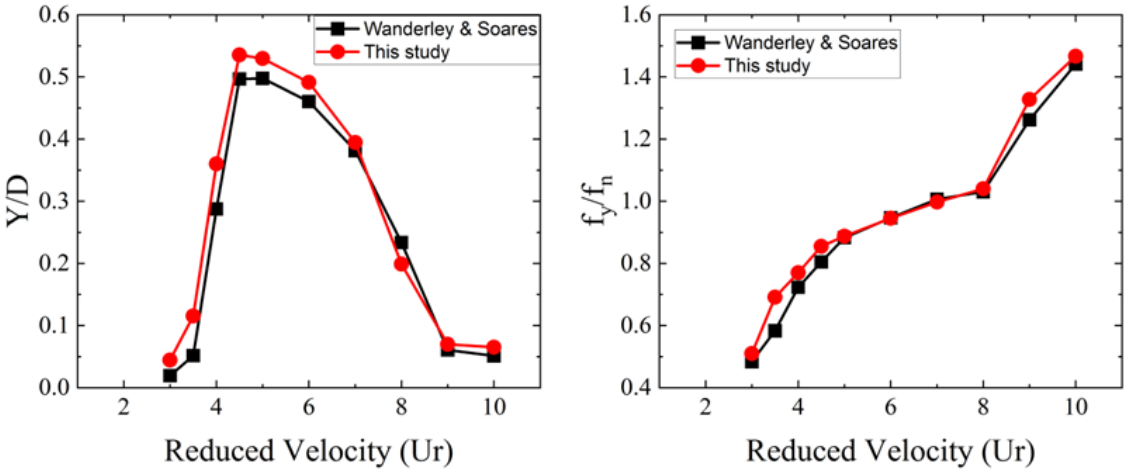

Fig. 2: Model validation at Re = 100 with $m^* = 1.88$ and $\zeta = 5.42\times10^{-3}$.

3. Results & Discussion

Fig. 3a presents the root mean square (RMS) of nondimensional vibration amplitude (Y/D), while Fig. 3b displays the ratio of vibration frequency to the natural frequency of the structure (fy/fn). The results of the slitted cylinders having slit ratios (S/D) of 0.1 and 0.2 are compared with the solid cylinder (S/D = 0) across varying Ur (2 – 10). The overall pattern of Y/D concerning Ur remains constant with and without the slit. As Ur increases, the vibration amplitude goes up, peaking at Ur = 6, and declines with further increments in Ur. Notably, at Ur = 6 the cylinder experiences substantial vibrations due to the lock-in condition, where fy/fn = 1. Comparing to the solid cylinder, introducing a 10% slit lowers the highest amplitude by 5.16%, whereas a 20% slit leads to a significant 34.27% decrease. These results suggest that a 10% slit is insufficient to significantly disrupt downstream vortex shedding patterns, while a 20% slit enhances the disturbance by letting larger amount of fluid to pass through it disrupting the wake.

With increasing Ur, fy/fn generally rises and reaches 1, indicating lock-in, especially at reduced velocity of 6. At S/D = 0 & 0.1, the cylinder stays in lock-in until reduced velocity of 8, whereas the cylinder with S/D = 0.2 only experiences lock-in at reduced velocity of 6. Beyond this point, the cylinder exits the lock-in condition, and fy/fn continues to increase with rising Ur.

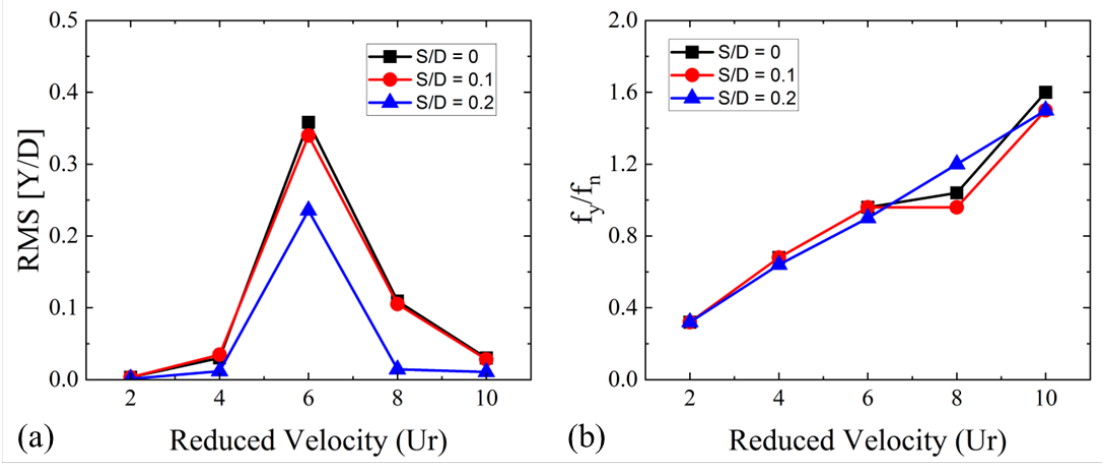

Fig. 3: (a) Root mean square (RMS) of dimensionless vibration amplitude (Y/D), and (b) vibration frequency normalized with the natural frequency (f_y/f_n).

In Fig. 4a, the root mean square (RMS) of the coefficient of lift (C_L) is displayed. The periodic shedding of shear layers from the surface of the cylinder results in a periodically fluctuating lift force. Observing Fig. 4a, it becomes apparent that a 10% slit causes a slight deviation in C_L but increasing the slit width to S/D = 0.2 leads to a significant variation in C_L.

The C_L for solid cylinder and the cylinder with S/D = 0.1 is comparable, exhibiting an increasing trend as Ur increases increases until reaching max at Ur = 4. Subsequently, there is a decline in C_L, reaching a minimum at Ur = 8, followed by another rise on Ur = 10. Contrasted with the cylinder with no slit, the root mean square of C_L is lower for S/D = 0.1 at Ur = 2. Max occurs at Ur = 4 with a similar value of C_L for both S/D = 0 and 0.1. At high Ur values (6 & 8), the lift coefficient for the 10% slitted cylinder surpasses that of the solid cylinder.

The lift coefficient for a cylinder with a slit size of S/D = 0.2, is considerably lower than both a solid cylinder and a cylinder with 10% slit at small Ur values (2 & 4), as well as at Ur = 10. The peak now shifts to Ur = 6, breaking from the Ur = 4 pattern seen in both solid and 10% slitted cylinders. At reduced velocity of 6, coefficient of lift for S/D = 0.1 and 0.2 is greater than solid cylinder by 41.6% and 70.8%, respectively. However, the max of C_L for cylinder with S/D = 0.2 appears to be 28% lower than that achieved by the cylinder with no slit. At reduced velocity of 8, the root mean square of C_L for S/D = 0.2 matches with the cylinder with no slit (S/D = 0).

Fig. 4b illustrates the behaviour of the root mean square (RMS) of the drag coefficient (C_D). The C_D pattern closely mimics that of Y/D, reaching its max at Ur = 6, the same point of maximum Y/D depicted in Fig. 3a. Introducing slits, denoted by rising S/D, brings down the mean C_D, as the slit forms a pathway for arriving flow, allowing it travel through and thereby curbing pressure drag. Augmenting the slit size reduces the size of the cylinder halves, subsequently diminishing drag as the flow encounters smaller obstacles.

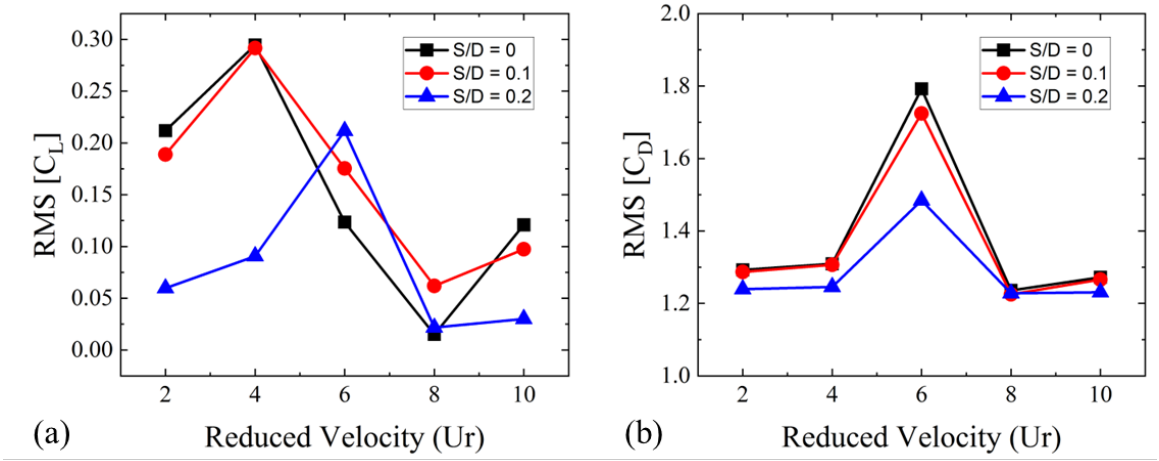

Fig. 4: Root mean square (RMS) of (a) coefficient of lift (C_L), and (b) coefficient of drag (C_D).

Fig. 5a displays the vortex shedding patterns at Ur = 6 & 8 through dimensionless vorticity contours. These conditions reveal a 2S vorticity pattern. Vorticity for both S/D = 0 & 0.1, exhibit striking similarity, indicating that the 10% slit has minimal impact on the flow behaviour. A vaguely altered pattern emerges at Ur = 8, hinting at a slower shedding of vortices for the solid cylinder compared to Ur = 6.

Fig. 5b clearly illustrates the impact of slit size (S/D) and Ur on Strouhal number (St). Remarkably, at Ur = 0 – 6, the Strouhal number dynamics for cylinder with no slit (S/D = 0) and cylinder with S/D = 0.1 remain indistinguishable. This underscores that the existence of a small size slit (S/D = 0.1), aligned with the flow, exerts no influence on Strouhal number during these conditions. However, as Ur escalates to high levels (8 & 10), the Strouhal number of a cylinder with S/D = 0.1 diverges from that of cylinder with no slit and aligns itself with the St of a cylinder with S/D = 0.2. As a result, the deduction can be made that a 10% slitted cylinder mimics the behaviour of a solid cylinder at Ur = 0 – 6 and exhibits characteristics of a 20% slitted cylinder at Ur = 8 – 10.

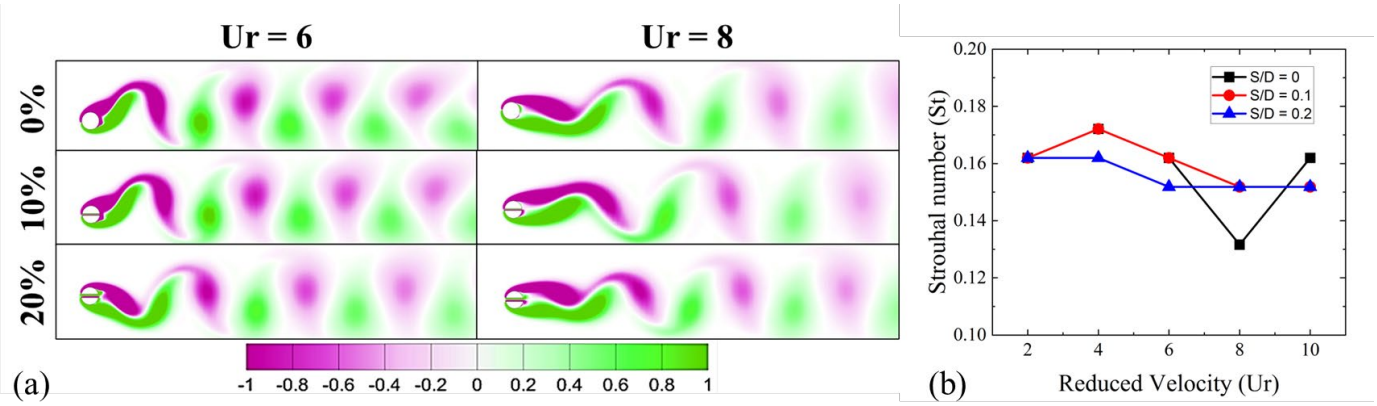

Fig. 5: (a) Vorticity contours at Ur = 6 & 8, and (b) Strouhal number for S/D = 0, 0.1, & 0.2.

4. Conclusions

A passive flow control technique was employed in this work by introducing a slit in the cylinder to alleviate developed forces and associated vortex-induced vibrations (VIV). The outcomes imply that the inclusion of a slit effectively diminishes drag & lift coefficients, while also mitigating VIV. In comparison to the cylinder with no slit, the introduction of a small slit (S/D = 0.1) results in a modest 5.16% reduction, and a comparatively larger slit (S/D = 0.2) leads to a substantial 34.27% decrease in the vibrational amplitude. While the cylinders with S/D = 0 and S/D = 0.1 remained in lock-in for Ur = 6 – 8, the cylinder with S/D = 0.2 experienced lock-in at Ur = 6 only. These findings suggest that a 10% slit may not significantly disrupt downstream vortex shedding patterns, while a 20% slit enhances disturbance by allowing a larger amount of fluid to pass through, disrupting the wake. These findings can provide valuable insights for engineers to design structures incorporated with slits to passively mitigate VIV, preventing potential breakdowns.

Nomenclature

c	damping coefficient	P	pressure
C_L	lift coefficient	Re	Reynolds number
C_D	drag coefficient	S	slit width
D	cylinder diameter	t	flow time
fn	natural frequency	u	velocity vector
F_L	lift force	Ur	reduced velocity
i, j	index notation	U_∞	free stream velocity
k	spring constant	Y, Ẏ, Ÿ	displacement, velocity, acceleration
m	virtual mass	ρ	density
$m_{cylinder}$	mass of the cylinder	ν	kinematic viscosity
m_{fluid}	mass of the displaced fluid	μ	dynamic viscosity
m*	mass ratio	ζ	damping ratio

Acknowledgements

This study is supported by Khalifa University of Science and Technology, Abu Dhabi, UAE, through Grant CIRA-2020-057. We gratefully acknowledge this support.

References

[1] U. Ali, Md. Islam, I. Janajreh, Y. Fatt, and Md. M. Alam, "Flow-Induced Vibrations of Single and Multiple Heated Circular Cylinders: A Review," *Energies*, vol. 14, no. 24, p. 8496, Dec. 2021, doi: 10.3390/en14248496.

[2] G. Liu, H. Li, Z. Qiu, D. Leng, Z. Li, and W. Li, "A mini review of recent progress on vortex-induced vibrations of marine risers," *Ocean Engineering*, vol. 195, p. 106704, Jan. 2020, doi: 10.1016/j.oceaneng.2019.106704.

[3] U. Ali, M. Islam, K. E. Kadi, and I. Janajreh, "Energy Harvesting from Wake-Induced Vibrations of a Downstream Cylinder in Tandem Arrangement," *Procedia Computer Science*, vol. 224, pp. 280–287, 2023, doi: 10.1016/j.procs.2023.09.038.

[4] R. Wang, D. Xin, and J. Ou, "Experimental investigation on suppressing circular cylinder VIV by a flow control method based on passive vortex generators," *Journal of Wind Engineering and Industrial Aerodynamics*, vol. 187, pp. 36–47, Apr. 2019, doi: 10.1016/j.jweia.2019.01.017.

[5] U. Ali, Md. Islam, I. Janajreh, Y. Y. Fatt, and Md. M. Alam, "Hydrodynamic and thermal behavior of tandem, staggered, and side-by-side dual cylinders," *Physics of Fluids*, vol. 36, no. 1, p. 013605, Jan. 2024, doi: 10.1063/5.0176710.

[6] M. Zhao, "A review of recent studies on the control of vortex-induced vibration of circular cylinders," *Ocean Engineering*, vol. 285, p. 115389, Oct. 2023, doi: 10.1016/j.oceaneng.2023.115389.

[7] I. Janajreh, H. Hassan, H. A. Abderrahmane, U. Ali, and M. Islam, "Numerical Analysis of Flow Over Slitted Cylinder and Experimental Validation Using Soap-Film Technique," in *ASME 2022 16th International Conference on Energy Sustainability*, Philadelphia, Pennsylvania, USA: American Society of Mechanical Engineers, Jul. 2022, p. V001T14A002. doi: 10.1115/ES2022-85827.

[8] U. Ali, Md. Islam, and I. Janajreh, "Influence of Surface Roughness on Heat Transfer and Flow-Induced Vibrations of a Circular Cylinder," in *Volume 5: Dynamics, Vibration, and Control*, Columbus, Ohio, USA: American Society of Mechanical Engineers, Oct. 2022, p. V005T07A040. doi: 10.1115/IMECE2022-94962.

[9] W.-L. Chen, X.-W. Min, and Y.-J. Guo, "Numerical simulation of passive-suction-jet control of flow over two side-by-side circular cylinders," *Ocean Engineering*, vol. 257, p. 111624, Aug. 2022, doi: 10.1016/j.oceaneng.2022.111624.

[10] G. Chen, W. Chen, X. Min, and D. Gao, "A coupled model for vortex induced vibration of a circular cylinder with and without passive-jet flow control," *Journal of Fluids and Structures*, vol. 110, p. 103541, Apr. 2022, doi: 10.1016/j.jfluidstructs.2022.103541.

[11] U. Ali, M. D. Islam, and I. Janajreh, "Flow over rotationally oscillating heated circular cylinder at low Reynolds number," *Ocean Engineering*, vol. 265, p. 112515, Dec. 2022, doi: 10.1016/j.oceaneng.2022.112515.

[12] A. Martín-Alcántara, V. Motta, A. Tarantino, and M. G. De Giorgi, "Design of a passive flow control solution for the mitigation of vortex induced vibrations on wind turbines blade sections as a response to extreme weather events," *Sustainable Energy Technologies and Assessments*, vol. 56, p. 103053, Mar. 2023, doi: 10.1016/j.seta.2023.103053.

[13] X.-W. Min, W.-L. Chen, Y.-J. Guo, and C. Chen, "Flow characteristics and mechanics of vortex-induced vibration of cable model under passive–suction–jet control," *Journal of Fluids and Structures*, vol. 116, p. 103811, Jan. 2023, doi: 10.1016/j.jfluidstructs.2022.103811.

[14] Y. Sarout, M. Islam, U. Ali, Y. Y. Fatt, and I. Janajreh, "Flow-Induced vibration and heat transfer enhancement in tandem cylinders: Effects of cylinder shape, corner radii, and spacing ratio," *Ocean Engineering*, vol. 285, p. 115397, Oct. 2023, doi: 10.1016/j.oceaneng.2023.115397.

[15] W.-L. Chen, G.-B. Chen, F. Xu, Y. Huang, D.-L. Gao, and H. Li, "Suppression of vortex-induced vibration of a circular cylinder by a passive-jet flow control," *Journal of Wind Engineering and Industrial Aerodynamics*, vol. 199, p. 104119, Apr. 2020, doi: 10.1016/j.jweia.2020.104119.

[16] G.-B. Chen, W.-L. Chen, W.-H. Yang, and D.-L. Gao, "Suppression of vortex-induced vibration of a box girder using active suction-jet slit," *Journal of Wind Engineering and Industrial Aerodynamics*, vol. 216, p. 104713, Sep. 2021, doi: 10.1016/j.jweia.2021.104713.

[17] D. Gao, Z. Deng, W. Yang, and W. Chen, “Review of the excitation mechanism and aerodynamic flow control of vortex-induced vibration of the main girder for long-span bridges: A vortex-dynamics approach,” *Journal of Fluids and Structures*, vol. 105, p. 103348, Aug. 2021, doi: 10.1016/j.jfluidstructs.2021.103348.
[18] U. Ali, H. Hassan, I. Janajreh, H. A. Abderrahmane, and Md. Islam, “Passive and active control for flow over a cylinder using a slit and validation with soap film technique,” *European Journal of Mechanics - B/Fluids*, vol. 98, pp. 279–291, Mar. 2023, doi: 10.1016/j.euromechflu.2022.11.003.
[19] M. Verma, A. Mishra, and A. De, “Flow characteristics of elastically mounted slit cylinder at sub-critical Reynolds number,” *Physics of Fluids*, vol. 33, no. 12, p. 123612, Dec. 2021, doi: 10.1063/5.0073368.
[20] H. Baek and G. E. Karniadakis, “Suppressing vortex-induced vibrations via passive means,” *Journal of Fluids and Structures*, vol. 25, no. 5, pp. 848–866, Jul. 2009, doi: 10.1016/j.jfluidstructs.2009.02.006.
[21] İ. Karasu, “Flow control over a diamond-shaped cylinder using slits,” *Experimental Thermal and Fluid Science*, vol. 112, p. 109992, Apr. 2020, doi: 10.1016/j.expthermflusci.2019.109992.
[22] T. Igarashi, “Flow Characteristics around a Circular Cylinder with a Slit : 1st Report, Flow Control and Flow Patterns,” *Bulletin of JSME*, vol. 21, no. 154, pp. 656–664, 1978, doi: 10.1299/jsme1958.21.656.
[23] L.-C. Hsu and C.-L. Chen, “The drag and lift characteristics of flow around a circular cylinder with a slit,” *European Journal of Mechanics - B/Fluids*, vol. 82, pp. 135–155, Jul. 2020, doi: 10.1016/j.euromechflu.2020.02.009.
[24] A. Mishra and A. De, “Suppression of vortex shedding using a slit through the circular cylinder at low Reynolds number,” *European Journal of Mechanics - B/Fluids*, vol. 89, pp. 349–366, Sep. 2021, doi: 10.1016/j.euromechflu.2021.06.009.
[25] Z. Yang, L. Ding, L. Zhang, L. Yang, and H. He, “Two degrees of freedom flow-induced vibration and heat transfer of an isothermal cylinder,” *International Journal of Heat and Mass Transfer*, vol. 154, p. 119766, Jun. 2020, doi: 10.1016/j.ijheatmasstransfer.2020.119766.
[26] U. Ali, M. Islam, and I. Janajreh, “Heat transfer and wake-induced vibrations of heated tandem cylinders with two degrees of freedom: Effect of spacing ratio,” *Physics of Fluids*, vol. 34, no. 11, p. 113612, Nov. 2022, doi: 10.1063/5.0124772.
[27] M. R. Lekkala *et al.*, “Numerical investigations of flow over wavy cylinders at sub-critical Reynolds number,” *Ocean Engineering*, vol. 269, p. 113501, Feb. 2023, doi: 10.1016/j.oceaneng.2022.113501.
[28] J. B. V. Wanderley and L. F. N. Soares, “Vortex-induced vibration on a two-dimensional circular cylinder with low Reynolds number and low mass-damping parameter,” *Ocean Engineering*, vol. C, no. 97, pp. 156–164, 2015, doi: 10.1016/j.oceaneng.2015.01.012.